Laboratori Nazionali di Frascati

LNF-92/018 (R)
30 Marzo 1992

V. Boffa, M. Cirillo, U. Gambardella, D. Di Gioacchino, G. Paternò:

SYMMETRIC TUNNELING JUNCTIONS WITH NbZr SUPERCONDUCTING THIN FILMS

Presented at the
3rd Inter. Workshop on
Tunneling Phenomena in High and Low T_c Superconductors
Capri, Italy – October 1–4 (1991)

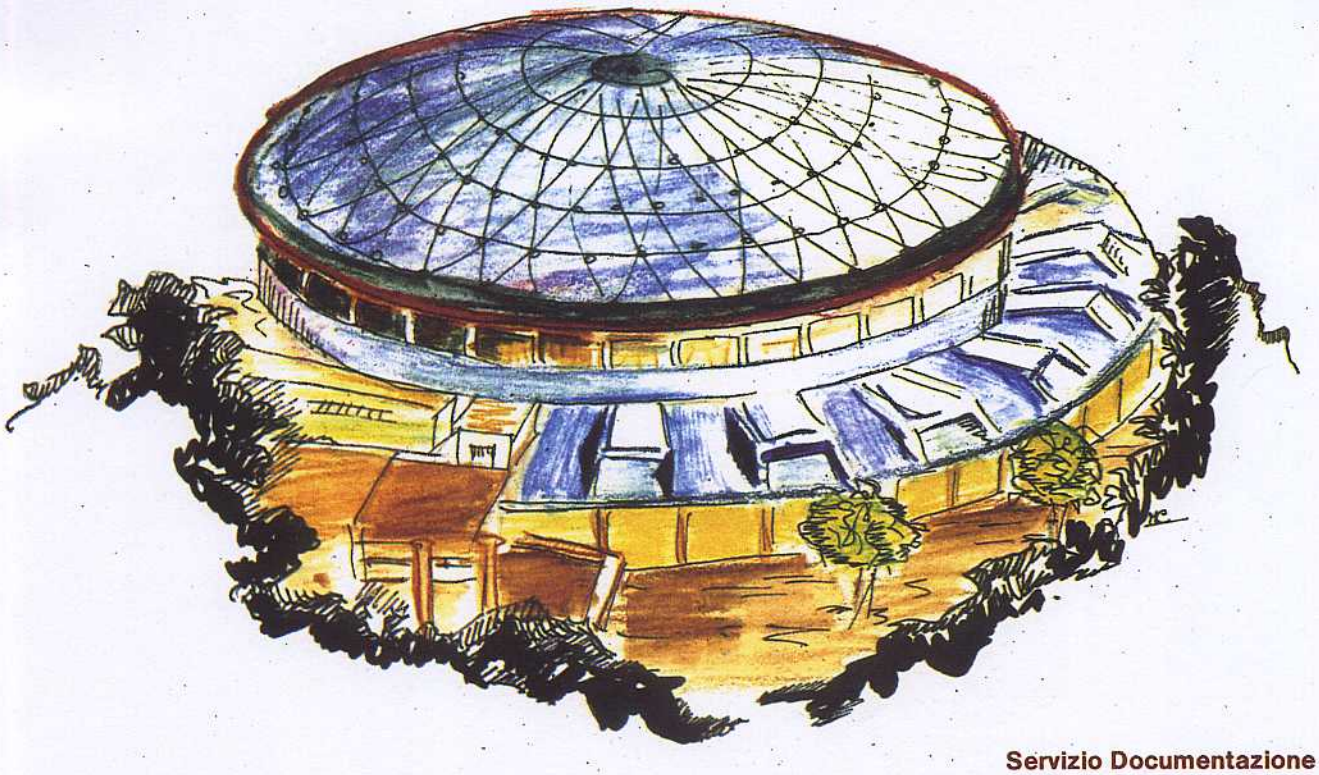

Servizio Documentazione
dei Laboratori Nazionali di Frascati
P.O. Box, 13 - 00044 Frascati (Italy)

LNF-92/018 (R)
30 Marzo 1992

V. Boffa, M. Cirillo, U. Gambardella, D. Di Gioacchino, G. Paternò:

SYMMETRIC TUNNELING JUNCTIONS WITH NbZr SUPERCONDUCTING THIN FILMS

Presented at the
3rd Inter. Workshop on
Tunneling Phenomena in High and Low T_c Superconductors
Capri, Italy – October 1–4 (1991)

INFN - Laboratori Nazionali di Frascati
Servizio Documentazione

LNF-92/018 (R)
30 Marzo 1992

SYMMETRIC TUNNELING JUNCTIONS WITH NbZr SUPERCONDUCTING THIN FILMS

D. Di Gioacchino, U. Gambardella
INFN-Laboratori Nazionali di Frascati, P. O. box 13, 00044RM Frascati, Roma, Italy

V. Boffa, G. Paternò
ENEA-CRE Frascati, P. O. box 65, 00044RM Frascati, Roma, Italy

and
M. Cirillo
Dipartimento di Fisica, Università di Roma Tor Vergata, 00173RM Roma, Italy

1. – INTRODUCTION

Refractory materials have received attention because of their potential application in thin film microwave devices or as coating materials in RF superconducting accelerator cavities[1,2]. Among these NbZr has been extensively studied for practical and fundamental physics-oriented purposes[3,4] because the $Nb_{1-x}Zr_x$ bulk system has a critical temperature[5] $T_c \approx 10.8$ K for x=0.25, and shows a weak dependence on the exact composition[6] which is important for device fabrication and reproducibility. Unfortunately a limited amount of data are available from NbZr thin films[6,7] fabricated by using different methods, i. e. co-sputtering from two cathodes or electron-beam evaporation; moreover in these cases the measured critical temperatures T_c was below 9 K.

Tunneling measurements on asymmetrical junctions (NbZr/Al/Al_2O_3/In or NbZr/Ox/Pb) have already been reported: these studies allowed a determination of the electron-phonon coupling factor[4] λ, and of the superconducting energy gap[3,8] Δ of the NbZr. So far, however, the data that have been reported are relative to tunnel junctions fabricated on thin NbZr foils. Moreover, in measurements of the energy gap in asymmetrical junctions having In or Pb as a counterelectrode there are temperature limitations due to the low T_c of the counterelectrode. The use of artificial barriers has been considered because of the poor insulating properties of the NbZr natural oxide. However, when using the NbZr as a coating material it is interesting to investigate its superconducting features resulting from NbZr oxide.

Work partially supported by CNR under the Progetto Finalizzato "Superconductive and Cryogenic Technologies"

In sect. 2 we discuss the fabrication of thin $Nb_{0.75}Zr_{0.25}/Ox/Nb_{0.75}Zr_{0.25}$ film tunnel junctions obtained by means of RF and DC magnetron sputtering. In sect. 3 we present the results of direct $\Delta(T)$ measurements in the temperature range (8.5-2.2) K; the $\Delta(T)$ behavior is compared with theoretical BCS results. In sect. 4 we discuss the microwave properties of the NbZr film as estimated from the Josephson self-resonances of the junctions (our junctions exhibit indeed Josephson effect). The estimate of the surface impedance is compared with previous data obtained for a $Nb_{0.75}Zr_{0.25}$ film measured in a cylindrical TE cavity[9].

2. - SAMPLES FABRICATION

Several films of $Nb_{0.75}Zr_{0.25}$ were sputtered on Corning glass 7059 or sapphire substrates and characterized from the point of view of critical temperature T_c. The magnetron cathode was provided with $Nb_{0.75}Zr_{0.25}$ target disc. Both RF and DC sputtering were used. The vacuum prior to deposition of the films was in the range (2-4) x 10^{-7} mbar. The RF sputtering were performed in 5 x 10^{-3} mbar of Ar, while the DC sputtering deposition were performed in a controlled Ar flow of 25 sccm, at a pressure of 1.5 x 10^{-3} mbar of Ar. Every deposition was precedeed by a pre-sputtering on a movable shield for several minutes. The substrate holder was sometimes heated up to 400 °C. The deposition rates were in the range (10-15) Å/s. The film thickness ranged between 3000 Å and 5000 Å.

In Fig. 1 we show resistance vs temperature for a $Nb_{0.75}Zr_{0.25}$ film deposited at 400 °C by DC sputtering at 14 Å/s on a Corning glass. The residual resistivity ratio between 300 K and 11 K is 1.47. The transition temperature T_c, measured with a calibrated thermometer, is shown in the inset: zero resistance is persistent up to T=10.4 K while biasing the sample at 10 μA. The critical temperature is lower than that reported for bulk samples, but it is well above data previously reported for films.

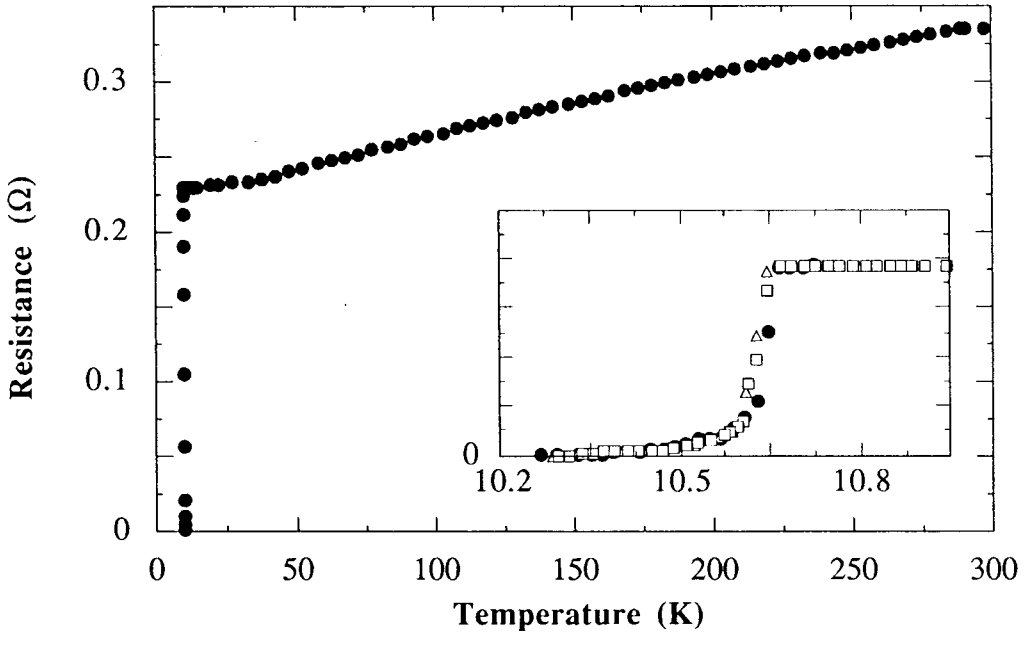

FIG 1 - R-vs-T behavior of NbZr #20 6000 Å thick, deposited on sapphire at 400 °C. The inset shows the transition region.

The cross-geometry of the tunnel junctions was defined by using metallic masks for the two depositions. The films width ranged from 100 to 200 μm. The lower electrodes were usually thinner than the upper ones in order to obtain a good overlapping of the films.

The oxide barriers were grown on the lower films by keeping the samples at room temperature in air for 17 hours minimum, however longer oxidation time, up to two days, gave similar results.

3. - SUPERCONDUCTING PROPERTIES

By using the standard four leads configuration the I-V curves of the tunnel junctions were recorded at different temperatures. Temperatures above the LHe temperature were attained by keeping the sample in cold He vapour, while temperatures lower than 4.2 K were obtained lowering the bath pressure. The biasing current was provided from a programmable current source and the corresponding voltage was measured by a high impedance differential nanovoltmeter. The measurements were managed by a computer which, recorded one data, when the temperatures were stable within ±20 mK for several minutes. The recording time of one I-V characteristic lasted less than 1 minute, allowing to neglect the slower temperature drift when measuring in cold He vapour. In Fig. 2 a typical I-V characteristic at 4.2 K is plotted. The tunnel resistance above the gap voltage is $R_{NN} \approx 0.22\ \Omega$, but the sub-gap resistance exhibits a rather low value indicating the existence of a significant leakage current. The latter fact is very likely due to the existence of microshorts in the oxide barrier at the junction edges, generated by the high deposition rate of the second electrode.

The energy gap Δ of the superconducting film is evaluated from the I-V characteristic of the tunnel junctions[10,11]. Better resolution in determining the Δ values was achieved with the numerically computed derivative of the I-V curve, shown in Fig. 2. The I-V characteristics of our junctions exhibited the typical behavior which indicate the presence of a proximity layer[12], thus we adopted the position of the second peak in the dI/dV-vs-V curves[4] as the gap voltage. In Fig. 3 we show the gap voltage as a function of the temperature for the sample G4Fd. In Fig. 3 we also show the BCS gap[13] (solid line) reduced to the measured $\Delta(0) \approx \Delta(2.43) = 1.45$ mV and $T_c = 8.5$ K. The largest gap voltage we obtained with sample G8Ed at 2.28 K was $\Delta(2.28) = 1.63$ mV: in this case to interpolate data a $T_c = 9.5$ K must be used. The agreement between the theory and experiment is satisfactory. The measured T_c of the junction electrodes is always higher than the T_c used to interpolate the Δ(T) data, supporting the hypothesis of a surface layer having depressed superconducting parameters. In view of this effect the "bulk" T_c is not significant for applications where the film surface is relevant.

Assuming that the Fermi velocity v_F of Nb and $Nb_{0.75}Zr_{0.25}$ are equal[14], we estimate the intrinsic BCS coherence length of our films $\xi_o = \hbar v_F / \pi \Delta(0)$ using the known values of Nb $\Delta_{Nb}(0) = 1.56$ meV and $\xi_{o_{Nb}} = 430$ Å. Thus, $\Delta(0) = 1.63$ meV corresponds to $\xi_o \approx 411$ Å. The value $v_F \approx 3.1 \times 10^7$ cm/s also leads to compute a mean free path $l = \tau v_F \approx 6.2$ Å, where $\tau \approx 2 \times 10^{-15}$ s comes out from the measured resistivity $1/\rho = (1/4\pi)\, \omega_p^2\, \tau$ and the reported $Nb_{0.75}Zr_{0.25}$ plasma frequency[14] $(\hbar \langle \omega_p^2 \rangle)^{1/2} \approx 8$ eV.

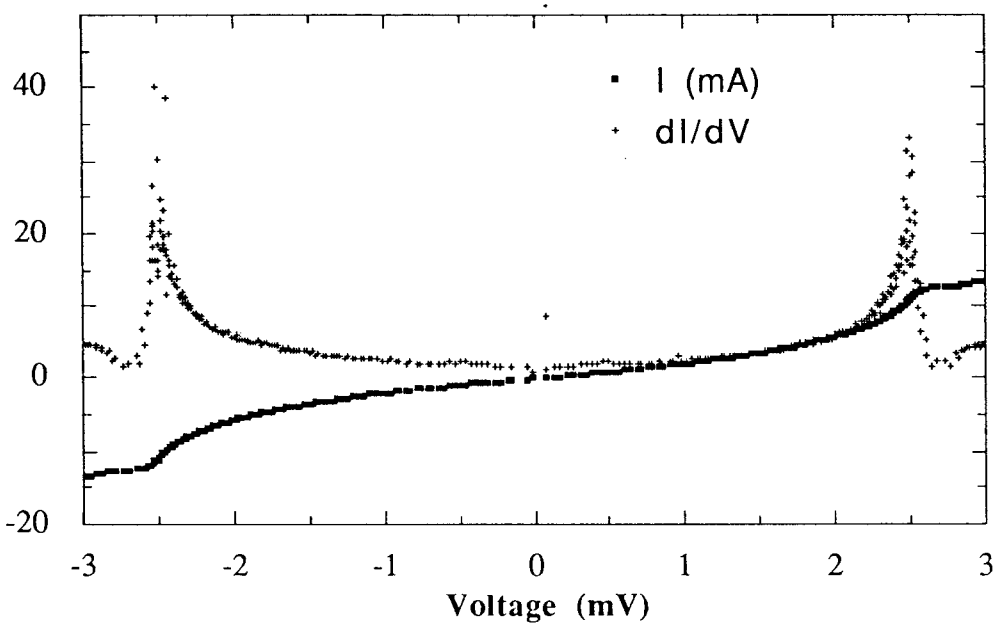

FIG. 2 - Typical I-vs-V characteristic of junction (solid square) and its corresponding derivative dI/dV (crosses).

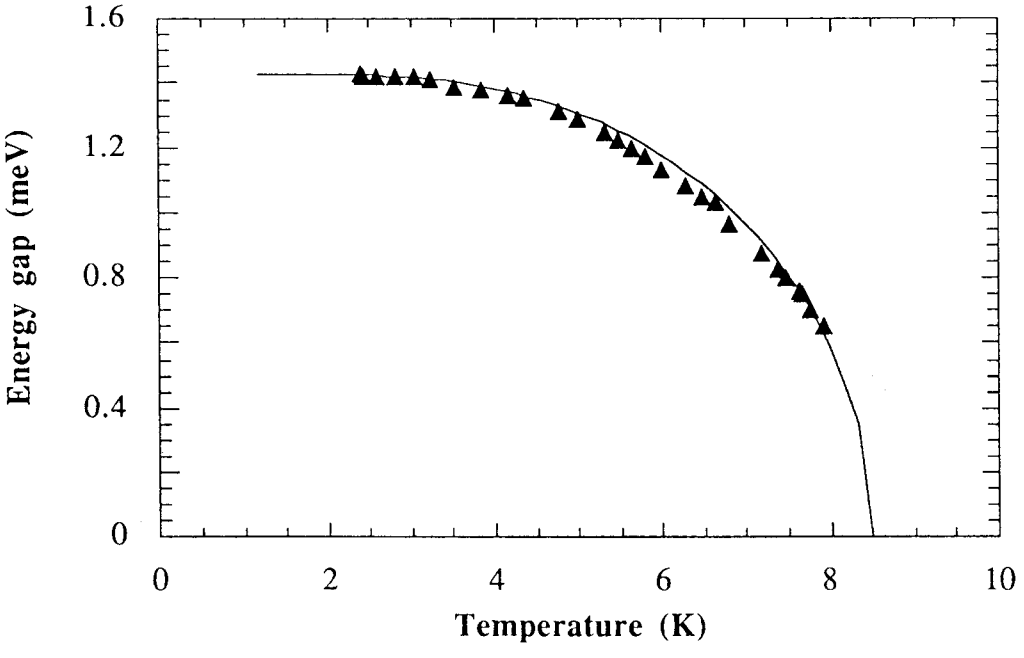

FIG. 3 - Temperature behavior of the measured gap voltage for the sample G4Fd (solid triangles). Solid line shows the theoretical BCS behavior.

4. – JOSEPHSON FEATURES

The magnetic penetration depth λ_{eff} in the $Nb_{0.75}Zr_{0.25}$ was estimated from the Josephson features exhibited by some tunnel junctions. Because of a very strong tendency to trap magnetic flux all the measurements on the Josephson junctions had to be performed in a magnetically shielded room. In Fig. 4 we report the I-V characteristic of the Josephson current recorded at 4.2 K in zero magnetic field on sample NG3Fu .

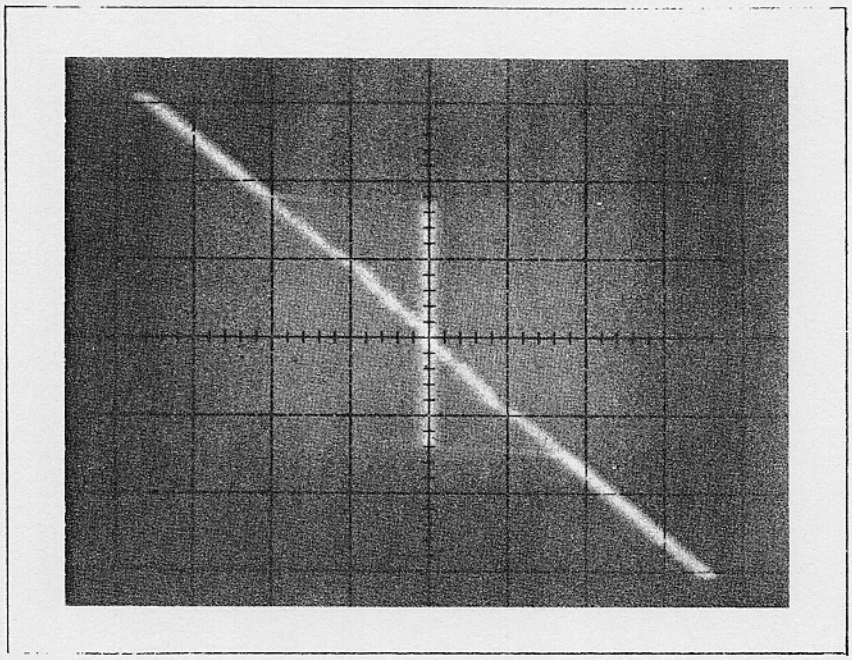

FIG. 4 – Sample NG3Fu: I-V characteristic of the Josephson current; x=100 μV/cm, y=200 μA/cm.

We measured the maximum Josephson current at 4.2 K as a function of the magnetic field; the field was provided by a long solenoid surrounding the junction. The magnetic field was perpendicular to the current flow in the junction, and parallel to the film surface. In Fig. 5 we show the maximum Josephson current behavior for sample G4Fu (crosses). The maximum Josephson current density at zero-field was $J_{c_o} \approx 2.8$ A/cm^2, being the junction dimensions (LxW) ≈ 240x220 μm^2. The total magnetic penetration depth $d=2\lambda_{eff}+t$, where t is the oxide thickness, is evaluated at $H^* = \phi_o/(Ld)$ when the first minimum of the Josephson current occurs. We estimate $H^* \approx 0.4$ gauss from Fig. 5, so that $d \approx 2\lambda_{eff} \approx 2300$ Å. In Fig. 5 a model of asymmetric current density distribution through the barrier has been used[15] to account for the non zero modulation of the maximum Josephson current. The theoretical behavior (dotted line) of the maximum Josephson current as a function of the reduced magnetic flux, for a junction having a length L where the current flows only through two regions $s_1=0.58$ L and $s_2=0.20$ L (see inset of Fig. 5) is in reasonable agreement with experimental data.

In Table I are listed typical quantities for some junctions which exhibited Josephson effect, such as the length L, the critical current density, the magnetic penetration depth λ_{eff} and the Josephson penetration depth λ_J, which was computed from the relation[16]:

$$\lambda_J = \sqrt{\frac{h}{4\pi e\, \mu_o d\, J_c}}$$

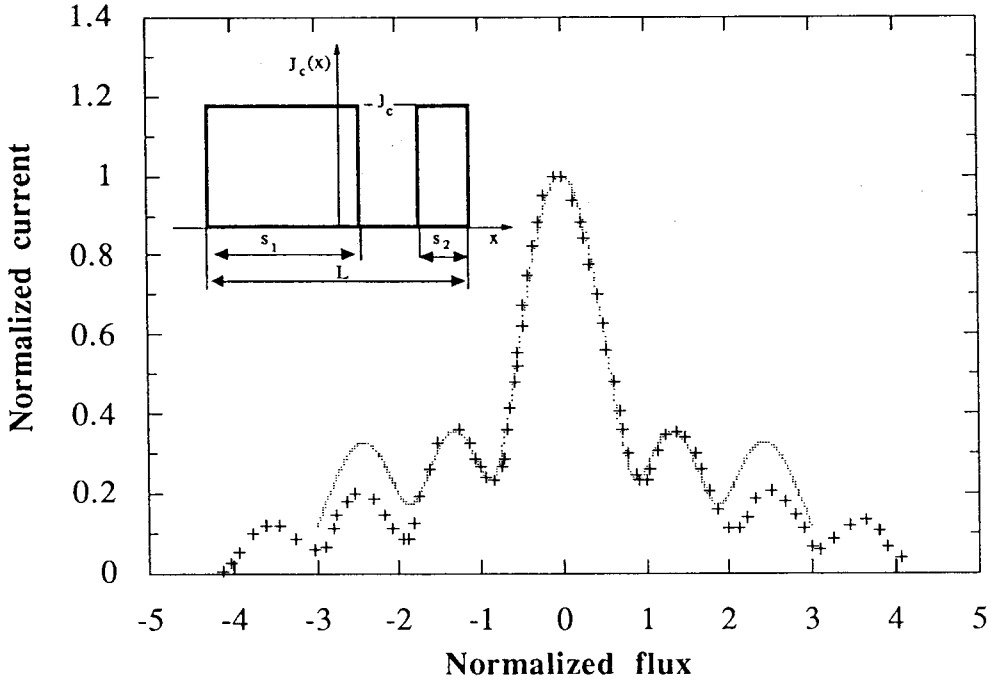

FIG. 5 – Maximum Josephson current amplitude as a function of the magnetic flux for sample G4Fu. Dotted line represents the theoretical computation of the Josephson current behavior for an asymmetrical current distribution like the one showed in the inset.

TABLE I - Properties of three Josephson tunnel junctions.

Sample	L (μm)	S (mm^2 x10^{-2})	J_c (A/cm^2)	λ_{eff} (Å)	λ_J (μm)
G4Fu	220±5	4.4±0.2	1.1±0.1	1150±120	317±18
G5Ed	240±5	4.6±0.2	2.8±0.1	917±92	226±11
G8Ed	250±5	5.0±0.2	7.8±0.4	n.a.	136±4

The presence of a weak magnetic field induced current steps at finite voltages on the I-V characteristic of some Josephson junctions. These current singularities (usually called Fiske steps) in "small" junctions are described by the Kulik[17] theory of self-resonances, where "small" means that the Josephson penetration depth λ_J is larger than the cross junction length L, i. e. $L/\lambda_J < 1$. By means of this theory the microwave surface impedance of the $Nb_{0.75}Zr_{0.25}$ films may be estimated. In fact the amplitude of the Fiske steps is related to the surface impedance of the films[18,1], in a way that depends on the junction quality factor Q.

The theoretical dependence of the first self-induced resonance on the magnetic field, valid for small junctions with high Q, is given, in terms of the magnetic flux ϕ, by[19]:

$$I_1(\phi)=I_{c_o} J_o(\tfrac{a}{2})\, J_1(\tfrac{a}{2})\; F_1(\phi) \qquad (1)$$

where I_{co} is the maximum Josephson current, and J_o, J_1 respectively are the Bessel functions

of zero and first order. The parameter a is the first solution of the implicit equation[20]:

$$J_o(\frac{a}{2}) = \sqrt{\frac{a}{Z_1 F_1(\phi)}} \qquad (2)$$

In this expression Z_1 is proportional to the junction quality factor and $F_1(\phi)$ is the Kulik function derived for the case of uniform Josephson current. From Eqs. (1) and (2) it comes out that the ratio $I_1^M/(I_{co}F_1(\phi))$ vs $Z_1F_1(\phi)$, where the superscript M indicates the maximum step amplitude, is an universal function[20] independent of ϕ.

In Fig. 6 the magnetic field behavior of the 1st and the 2nd current steps, I_1 and I_2, of the junction G4Fu at 4.2 K are reported together with the Josephson maximum current I_J. In this way we found $I_1^M/(I_{co}F_1(\phi)) \approx 0.36$, larger than the theoretical 0.34 computed with Eq. (1). However considering, as previously done, the asymmetrical current distribution in the junction, we computed the factor $F_1(\phi)$ with Eq. (10) of ref. 15 using again $s_1=0.58$ L and $s_2=0.20$ L.

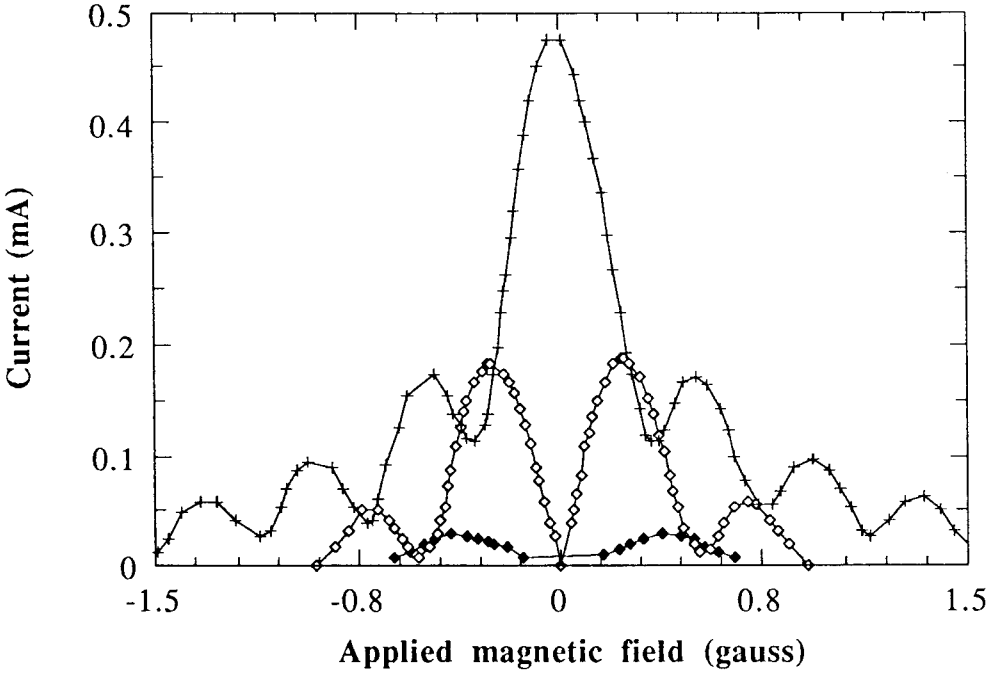

FIG. 6 – Sample G4Fu at 4.2 K: magnetic field behavior of the Josephson maximum current (crosses) 1st (open rhombs) and the 2nd (solid rhombs) current steps.

This resulted in a larger $F_1(\phi)$ and $I_1^M/(I_{co}F_1(\phi)) \approx 0.32$. In this way the value of Z_1 on the universal curve is ≈6. In Fig. 7 we show the experimental behavior of the first Fiske step for G4Fu; in the same figure we plot Eq. (1) computed by using the non uniform current distribution of $F_1(\phi)$ and for $Z_1=6$. Being the agreement satisfactory we compute the junction Q using:

$$Z_n = \left(\frac{L}{\lambda_j}\right)^2 \frac{Q_n}{\pi^2 n^2}$$

We find $Q_1 \approx 21$ for sample G4Fu at frequency $\nu_1 \approx 9$ GHz. Being the surface resistance[18] $R_s=X_s/Q$, where $X_s=2\pi\mu_o\lambda_{eff}\nu \approx 7.8 \times 10^{-3}\ \Omega$ is the imaginary part of the surface impedance,

we obtain $R_S \approx 3.7 \times 10^{-4}\ \Omega$ at 4.2 K and ν=9 GHz. This results does not agree completely with the value R_S=1.4 x $10^{-4}\ \Omega$ measured[9] at 4.2 K in a TE cavity at 7.8 GHz for a $Nb_{0.75}Zr_{0.25}$ film deposited on copper, even accounting for the frequency difference. We believe that the discrepancy may be mainly ascribed to the different techniques used for the measurement.

The assumption that the losses are almost entirely due to the surface resistance are supported by the simple estimate of the second major contribution to the losses[18]: the quasiparticle tunneling losses Q_p. This term is evaluated by means of $Q_p=2\pi\nu_1 R_d C_S WL$. At the dynamic resistance corresponding to the step voltage, $R_d \approx 1.5\ \Omega$, we estimated $Q_p \approx 3000$. This value is two orders of magnitude above the one evaluated from the surface resistance.

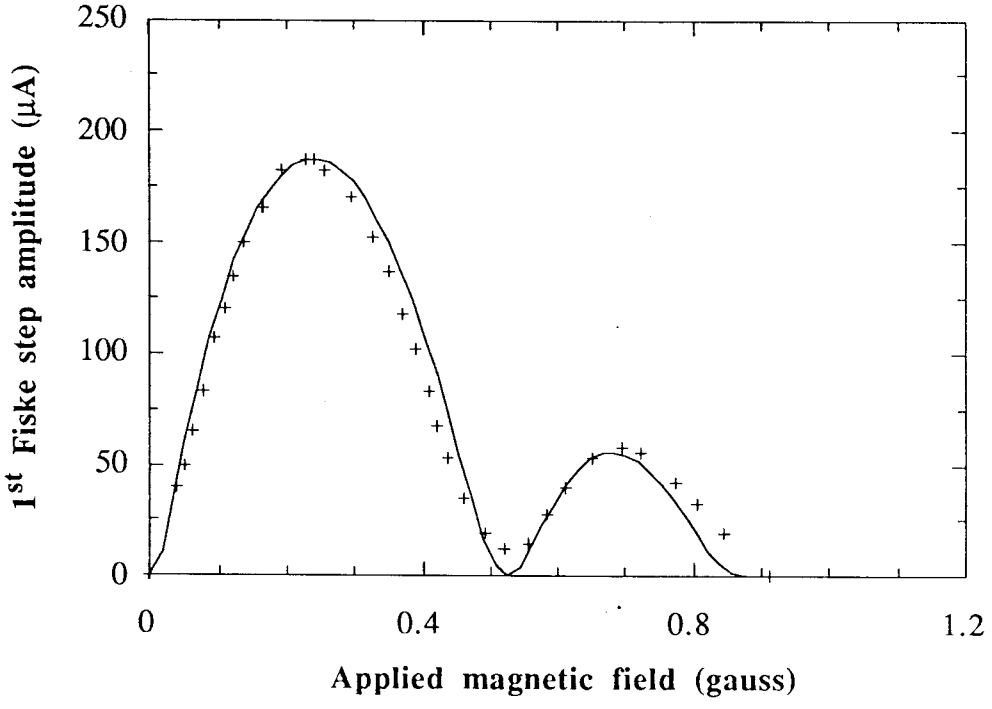

FIG. 7 – Experimental behavior of the first Fiske step for G4Fu (crosses); solid line is the plot of Eq. (1) computed with Z_1=6.

Finally in Table II we list the voltages V_n corresponding to the maximum Fiske amplitude, the Josephson frequency $\nu_n=2eV_n/h$, the speed of the electromagnetic field in the junction $\bar{c}=\nu_n\, 2L/n$, and the junction specific capacitance $C_S=\varepsilon_r\varepsilon_o/t$. The ratio ε_r/t is computed from $\bar{c}/c=(t/\varepsilon_r d)^{1/2}$.

Table II - Measured microwave quantities of the junctions.

junction	n	V_n (μV)	ν_n (GHz)	$\bar{c}/c$ x10^{-2}	C_S (F/m^2)
G4Fu	1	18	9	1.3	0.22
G4Fu	2	36	18	1.3	0.22
G5Ed	1	16	8	1.3	0.29
G5Ed	2	32	16	1.3	0.29

5. - CONCLUSION

In order to investigate the superconducting properties of $Nb_{0.75}Zr_{0.25}$ we have fabricated several symmetrical $Nb_{0.75}Zr_{0.25}/Ox/Nb_{0.75}Zr_{0.25}$ tunnel junctions by using thin film technology. In spite of the very simple fabrication process we were able to get junctions which showed tunneling characteristics useful for extensive gap measurements. The temperature behavior of the energy gap is in reasonable agreement with the BCS theory. In addition by means of Josephson tunneling we have also estimated the magnetic penetration depth and the microwave surface resistance of $Nb_{0.75}Zr_{0.25}$ thin films.

ACKNOWLEDGEMENTS

The authors are indebted with Prof. R. Vaglio, University of Salerno, for helpful discussions and suggestions, and with Mr. U. Baffi and L. Di Virgilio for their invaluable technical assistance.

REFERENCES

1. A. M. Cucolo, A. Nigro, R. Vaglio, *J. Low Temp. Phys.* **69** 5/6, 363 (1987).
2. C. Benvenuti, N. Circelli, M. Hauer, W. Weingarten, *IEEE Trans. on Mag.* **MAG-21** 2, 153 (1985).
3. E. L. Wolf, R. J. Noer, *Solid State Comm.* **30**, 391 (1979).
4. E. L. Wolf, R. J. Noer, G. B. Arnold, *J. Low. Temp. Phys.* **40** 5/6, 419 (1980).
5. J. K. Hulm, R. D. Blaugher, *Phys. Rev.* **123** 5, 1569 (1961).
6. H. J. Spitzer, *J. Vac. Sci. Technol.* **7** 5, 537 (1970).
7. R. Delesclefs, Ø. Fischer, *J. Low Temp. Phys.* **53** 3/4, 339 (1983).
8. I. Dietrich, *Phys. Lett.* **9** 3, 221 (1964).
9. D. Di Gioacchino, P. Fabbricatore, S. Frigerio, U. Gambardella, R. Musenich, R. Parodi, G. Paternò, S. Rizzo, C. Vaccarezza, *IEEE Trans. on Mag.* **MAG-27** 2, 1299 (1991).
10. I. Giaever, *Phys. Rev. Lett.* **5** 4, 147 (1960).
11. J. Nicol, S. Shapiro, P. H. Smith, *Phys. Rev. Lett.* **5** 10, 461 (1960).
12. G. B. Arnold, *Phys. Rev.* **B 18**, 1076 (1978).
13. B. Muhlschlegel, *Z. Physik* **155**, 313 (1959).
14. L. R. Testardi L. F. Mattheiss, *Phys. Rev. Lett.* **41** 23, 1612 (1978).
15. G. Paternò, A. M. Cucolo, R. Vaglio, *J. Appl. Phys.* **60** 4, 1455 (1986).
16. A. Barone and G. Paternò, *Physics and Applications of the Josephson Effect* (John Wiley & Sons, 1982) p. 70.
17. I. O. Kulik, *Sov. Phys. - Tech. Phys.*, **12** 1, 111 (1967).
18. T. C. Wang, R. I. Gayley, *Phys. Rev. B* **18** 1, 293 (1978).
19. Y. S. Gou, R. I. Gayley, *Phys. Rev. B* **10** 11, 4584 (1974).
20. A. Barone and G. Paternò, *Physics and Applications of the Josephson Effect* (John Wiley & Sons, 1982) p. 259.